Contents lists available at ScienceDirect

Journal of Nuclear Materials

journal homepage: http://ees.elsevier.com

ZrN coating as diffusion barrier in U(Mo) dispersion fuel systems

A. Leenaers [a,*], B. Ye [b], J. Van Eyken [a], S. Van den Berghe [a]

[a] Nuclear Materials Science Institute, SCK•CEN, Boeretang 200, 2400 Mol, Belgium
[b] Chemical and Fuel Cycle Technology Division, Argonne National Laboratory, 9700 S. Cass Ave. Lemont, IL 60439, USA

ARTICLE INFO

Article history:
Received 11 February 2021
Received in revised form 29 March 2021
Accepted 30 March 2021
Available online xxx

ABSTRACT

The control of the interaction between the U(Mo) fuel phase and the Al matrix is one of the challenges of dispersion fuel plate development for research reactors. Given the specific properties of this interaction layer, larger amounts of it in the meat could lead to a reduction of the plate mechanical integrity and thermal conductivity, eventually leading to pillowing. The SELENIUM project showed that by depositing a ZrN coating on the surface of the U(Mo) fuel particles, the amount of formed U(Mo)-Al interaction layer is limited but still present. Microstructural analysis performed on the as fabricated coating and fresh fuel plates containing ZrN coated U(Mo) dispersed in an Al matrix, revealed that the coating gets damaged during plate production. The post irradiation examinations (PIE) of the ZrN coated U(Mo) fuel plates, from the SELENIUM and SEMPER FIDELIS experiments, show how the U(Mo)-Al interaction layer is formed - only at those locations where the coating is missing or damaged - and the evolution of coating microstructure during irradiation. As a remedy, to further reduce the amount of interaction layer formed, the use of an Al-Si matrix was proposed based on the higher affinity of Si for U compared to the affinity of Al for U. PIE of a fuel plate consisting of ZrN coated U(Mo) dispersed in an Al-Si matrix irradiated in the SEMPER FIDELIS experiment, clearly demonstrates the benefit of adding Si to the matrix.

1. Introduction

Low enriched U(Mo) has been selected as a viable candidate to replace the high enriched fuel currently still used in several high performance research reactors (HPRR). Two U(Mo) based fuel systems are being considered: a dispersion in which atomized U(Mo) particles are dispersed in an Al matrix or monolithic where a U(Mo) foil is clad with Al sheets. In the build up to qualification of this new fuel, several irradiation experiments have been performed. It was found that both dispersion and monolithic fuels suffer from detrimental interaction between the U(Mo) fuel and Al matrix or Al cladding that lead to poor in-pile behavior of the fuel systems. To limit or even eliminate the formation of such a deleterious U(Mo)/Al interaction layer, the application of a diffusion barrier was evaluated. The role of a diffusion barrier is to prevent or slow down the inter-diffusion of the two materials in contact. Therefore, to be effective, a good diffusion barrier requires inertness with respect to adjacent materials.

In the case of the monolithic fuel system, a pure zirconium layer is employed for the purpose of controlling the U(Mo)-Al interdiffusion at the foil/cladding interface during both plate fabrication and irradiation. A barrier thickness of ~25 μm is usually selected to exceed the maximum fission fragment recoil range (~9 μm in Zr). For U(Mo) dispersion fuel the application of coatings directly on the powder particles surface by physical vapor deposition (PVD) [1], was expected to limit or possibly even avoid the interaction between the fuel and the Al matrix altogether. Even if the fission products are not stopped, the diffusion barrier does prevent the recoil atoms of the fuel phase and the matrix to reach each other, thereby preventing interaction. The SELENIUM (Surface Engineering of Low ENrIched Uranium-Molybdenum) fuel development project of SCK•CEN [2] consisted of the production, irradiation and post-irradiation examination of 2 flat, full size plates containing coated U(Mo) atomized powders dispersed in a pure Al matrix. Next to silicon, ZrN was selected as coating material as it is metallurgically inert towards U(Mo) and Al. The choice of ZrN was also based on the experience of the Russian MIR irradiated mini rods containing ZrN coated U(Mo) [3]. The post irradiation examination (PIE) clearly showed the positive effect of the coatings; for both Si and ZrN coated fuel a virtual absence of reaction between the U(Mo) and the Al is observed up to high fission densities after which a U(Mo)/Al interaction layer has formed. Even though both coatings have a clear effect on the kinetics of interaction layer formation, their behavior and evolution is completely different under irradiation [4]. Whereas the Si coating interacts with U(Mo) during plate production and the resulting U-Si rich interaction layer intermixes with the Al matrix during irradiation, the

* Corresponding author.
E-mail address: aleenaer@sckcen.be (A. Leenaers)

https://doi.org/10.1016/j.jnucmat.2021.153000
0022-3115/

ZrN layer seems to remain unaffected, i.e. it did not react with the fuel particles or the matrix, during plate production. However, also in the case of the ZrN layer, still the deleterious U(Mo)/Al interaction layer was formed and the degradation of the coating with increasing burnup was observed. Extensive microstructural characterization on fresh and (ion) irradiated ZrN coatings has been performed in order to understand its in-pile behavior [4–11].

Following the SELENIUM irradiation, several irradiation experiments using ions [6,12,13] have been performed on coated particles. The neutron irradiation called SEMPER FIDELIS was performed by the European Consortium HERACLES[1] at BR2 (Mol, Belgium) and aimed on investigating the fuel swelling phenomenon and effects of coatings while the sister irradiation EMPIrE (European Mini-Plate Irradiation Experiment), by ANL/INL at ATR (Idaho, US), had a focus on the in-pile behavior of various ZrN coated U(Mo) powder batches, produced by different technological processes (physical vapor deposition or atomic layer deposition processes) [14–16].

This paper gives an overview of the microstructural analyses performed on as fabricated ZrN coatings deposited by PVD as well as the examination on fresh fuel plates containing ZrN coated U(Mo) particles. The behavior of the ZrN coating under irradiation as previously observed in the SELENIUM irradiation is confirmed by comparing the PIE results of some of the SEMPER FIDELIS plates to the existing results.

2. Fabrication history

The U(Mo) powders used are prepared by an atomization process developed by the Korea Atomic Energy Research Institute (KAERI) [17]. This method results in spherical particles that show cellular microstructure, which is usually found in rapidly cooled alloys that have a substantial liquidus-solidus gap. The thick Mo deficient U(Mo) layers defining the cell boundaries [18], are known to directly reduce the stability of the γ-U(Mo) structure [19,20]. It is at these cell boundaries that restructuring (polygonisation) of the fuel and initial precipitation of the fission gas is observed [21,22]. The PIE of the SELENIUM plates (and plates from prior irradiation campaigns) clearly showed that restructuring can be correlated to an increase in swelling rate of the fuel plate. A heat treatment of the powder to homogenize the Mo content and promote grain growth, was suggested as procurement to delay restructuring and as such the increase in fuel swelling rate. The U(Mo) powder of the SELENIUM U7MD1231 plate was not heat treated (NHT) while the fuel for the SEMPER FIDELIS FIDJ0204 plates were annealed (HT) at 1000°C for 1 h (Table 1).

Application of the coating on U(Mo) particles was performed using magnetron sputtering, a PVD method where atoms that are ejected from a target traverse the vacuum and are deposited atomistically on a substrate to form a thin layer. In 2009 SCK CEN and the University of Ghent developed the STEPS&DRUMS (''Sputtering Tool for Engineering Powder Surfaces'' & ''Deposition Reactor for Uranium based Model Systems'') setup [1] . The reactor is a vacuum vessel with at one end a rotating drum to coat particles. The reactor is pumped down to the 10^{-6} mbar range and high-purity Ar gas is admitted in the chamber. In the case of ZrN deposition from a Zr target, high purity nitrogen is added. TRIM calculations were performed to estimate the required diffusion barrier thicknesses, based on a ballistic approach and it was concluded that a diffusion barrier of ~1μm ZrN should be capable of avoiding the recoiled Al and U atoms from interacting, thus effectively preventing IL formation [18].

The thickness of the ZrN coating was measured from the scanning electron microscopy (SEM) images at four positions on 50 randomly chosen fuel particles. A homogeneous coating with an average thickness as displayed in Table 1, was measured. The high standard deviation is expected due to the absence of stereographic corrections. The thickness of the coating layer for large fuel kernels will of course be smaller than on those particles having a small diameter.

Table 1.
A summary of the meat characteristics of the fuel plates under investigation.

Experiment	Plate Id	Powder Type	Matrix Type	Coating thickness(μm)	Heat treatment of the U(Mo) particles
SELENIUM	U7MD1231	ZrN coated	Al	1.15 ± 0.31	NHT
SEMPER FIDELIS	FIDJ0204	ZrN coated	Al	0.84 ± 0.25	HT

All fuel plates were fabricated by FRAMATOME CERCA using the standard 'picture frame' plate production process and were subsequently irradiated in the BR2 reactor of SCK CEN.

3. Irradiation history

The SELENIUM plate U7MD1231 was irradiated for 3 cycles with a maximum power at beginning-of-life (BOL) close to 470 W/cm^2. Due to the absence of burnable neutron absorbers, there is a gradual reduction in power with burnup, reaching a value of around 250 W/cm^2 at end-of-life (EOL) The plate attained an average burn-up of ~48 % ^{235}U and a local maximum burn-up just below 70%^{235}U (Table 2).

The irradiation history of the SEMPER FIDELIS plate FIDJ0204 is similar to the SELENIUM plate, except that FIDJ0204 remained in the reactor for an additional cycle. As a result, an average and maximum burnup of respectively ~57 and ~82% ^{235}U was attained (Table 2).

4. Microstructural analysis of as fabricated ZrN coatings

4.1. Coated U(Mo) powder

To obtain a homogeneous coating, the deposition of the ZrN layer on the U(Mo) powder was performed in a rotating drum system (STEPS&DRUMS), keeping the particles in constant motion during the sputtering process [1]. The use of this system has a significant impact on the final microstructure of the coating.

The high magnification scanning electron microscopy (SEM) image (Fig. 1), shows a 1 μm homogeneous thick ZrN coating deposited on a U(Mo) particle. The coating is composed of a dense layer of a few tens of nanometer followed by a layer showing a porous columnar, cauliflower microstructure.

The growth and final microstructure of a sputtered coating is predominately controlled by the deposition pressure, amount of surface and volume diffusion, degree of oblique incidence and the amount of ion bombardment. As the surface area of a spherical particle, that needs to be exposed to the vapor flux, is four times larger than a planar substrate having the same size of the circular cross-section of the microsphere [23], the effective deposition rate is very low (~0.04 nm/s). Furthermore the need for constant motion prevents the control of the microsphere substrate temperature, meaning that the deposition occurred at low temperature. For randomly moving spheres, the deposition flux is received under an oblique angle of 45° incidence as a result of the rapid time average by the moving microsphere over all deposition angles [23]. This oblique incidence has the effect of promoting Zone 1 of the structure zone model (SZM) defined by Movchan and Demchishin [24]. In this model, zone 1 structures are columnar units separated by voided boundaries that are several nanometers wide. They arise from shadowing effects and very limited adatom motion. This leads to a

[1] HERACLES is composed of AREVA-CERVA, CEA, ILL, SCK•CEN and TUM

Table 2.
Fabrication and irradiation history of the SELENIUM and SEMPER FIDELIS fuel plates.

Experiment	Plate ID	Cycle	max HF at BOCW/cm ^{2}	Max Burnup at EOC% ^{235}Uf/cm ^{3}	Mean Burnup at EOC% ^{235}Uf/cm ^{3}	Effective full power days
SELENIUM	U7MD1231	02/2012	466	26.8	15.7	27
				1.9E+21	1.1E+21	
		03/2012	381	54.8	35.5	21
				4.1E+21	2.6E+21	
		04/2012	290	69.6	47.5	21
				5.3E+21	3.5E+21	
SEMPER FIDELIS	FIDJ0204	03/2018	437	34.3	20.5	26
				2.5E+21	1.5E+21	
		04/2018	324	53.0	32.2	21
				4.0E+21	2.3E+21	
		05/2018	304	66.5	42.3	21
				5.4E+21	3.2E+21	
		06/2018	301	82.4	56.7	28
				6.5E+21	4.3E+21	

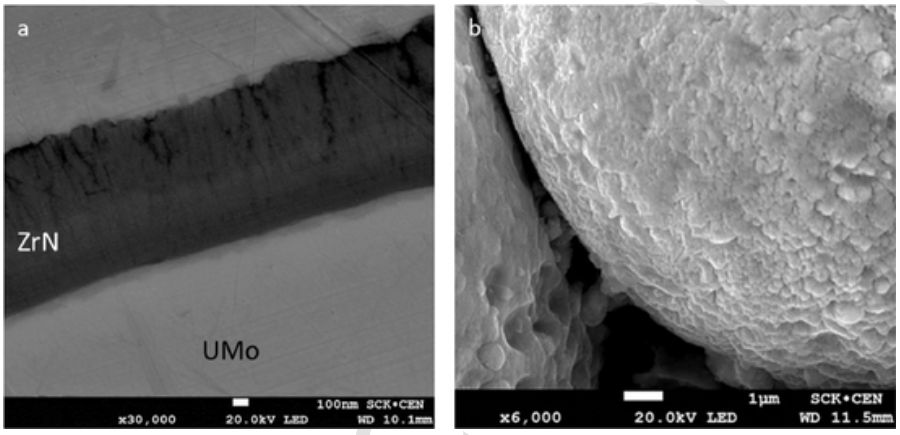

Fig. 1. Secondary electron image of a PVD deposited ZrN coating on U(Mo) showing the porous columnar cauliflower microstructure of the layer : a) in cross section b) on the outer surface of the coated fuel particle.

structure that takes on a cauliflower type appearance [25] as observed in Fig. 1.

The most important consequences, with regards to the prevention of the U(Mo)-Al interaction, of the columnar-void microstructure can be the lower density of the coating, lower thermal conductivity and the porosities could serve as a pathway for Al diffusion towards the U(Mo) fuel.

X-ray reflectivity (XRR) measurements were performed on a comparable ZrN coating deposited on a flat surface (Si wafer) to assess the density of the layer. It was found that the crystalline ZrN coating has a density of 6.82 g/cm^3, indeed a little lower than the theoretical density of 7.09 g/cm^3.

The X-ray diffraction pattern of measured ZrN coated as atomized powder (Fig. 2b) reveals that the coating consists of a crystalline (cubic cF8 structure) ZrN phase with a crystal sturcture that is consistent with a nominally stoichiometric ZrN reference [6,7]. The broad peaks of the ZrN phase are consistent with the nanoparticles observed in Fig. 1. A crystallite size ranging between 5 nm [26] and several tens of nanometers [7] is reported. The other phases found are UO_2 and UC and known contaminants of the U(Mo) powder (Fig. 2a insert). A study by He et al. [9] confirmed the nominal stoichiometry of the ZrN coating. Using atom probe tomography (APT). Measurements performed on the as fabricated coating resulted in 49.9 ± 0.9 % Zr, 48.9 ± 0.9 % N and 0.3 ± 0.05 % O.

4.2. Coated heat treated U(Mo) powder

The annealing of the U(Mo) powders, to homogenize the Mo content and induce grain growth, is performed in a Pyrotherm furnace equipped with an horizontal (stationary) ceramic tube. The powder is loaded in an Al_2O_3 crucible and surrounded by tantalum foil for oxygen gettering. The crucible is placed in the tube, which is subsequently sealed off and continually flushed with argon. Quenching is done by retracting (under Ar atmosphere) the crucible from the heated zone. Phase identification performed on the XRD scans of the heat treated U(Mo) powder show that in addition to uranium oxide and uranium carbide (both contaminates of as atomized U(Mo)), uranium nitride had formed (Fig. 2c). This indicates that the powder was exposed to air (contamination of the Ar atmosphere). Scanning electron microscopy in combination with energy dispersive X-ray analysis (SEM/EDX) indeed shows that on the surface of the fuel kernels, a contamination layer has formed (Fig. 3).

It should be noted that not all heat treated particles are affected and the thickness of the contamination layer is variable. It is assumed that the position of a particle in the powder batch in the crucible determines the extent to which it was exposed to the atmosphere.

The XRD scan in Fig. 2d and the X-ray distrubition maps of the outer surface of a coated, annealed U(Mo) particle (Fig. 4) both clearly show that the contamination layer does not affect the ZrN coating. A stoichiometric ZrN phase is measured and no interdiffusion between coating and contamination layer is observed.

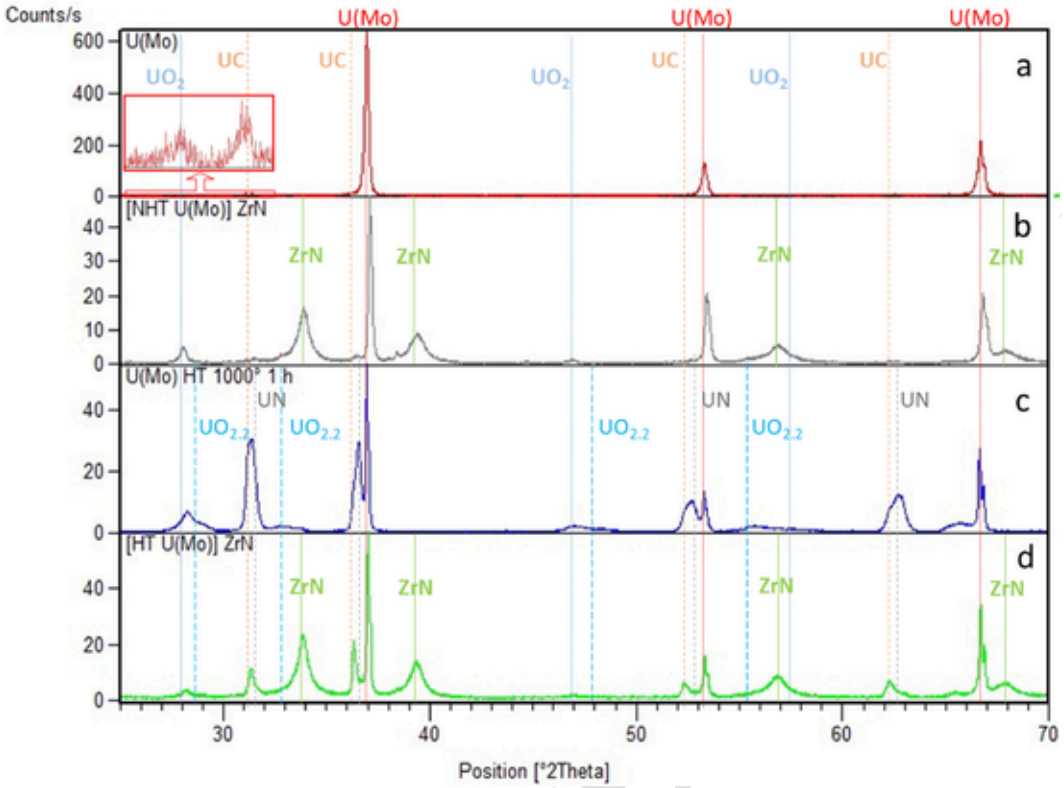

Fig. 2. Measured X-ray diffraction pattern of a) U(Mo), b) ZrN coated U(Mo), c) heat treated U(Mo) and d) ZrN coated heat treated U(Mo) particles and the reference pattern JCPDS 00-036-0089 for UO_2, JCPDS 00-047-1879 for $UO_{2.2}$, JCPDS00-032-1397 for UN, JCPDS01-073-1709 for UC and JCPDS 00-002-0956 for ZrN.

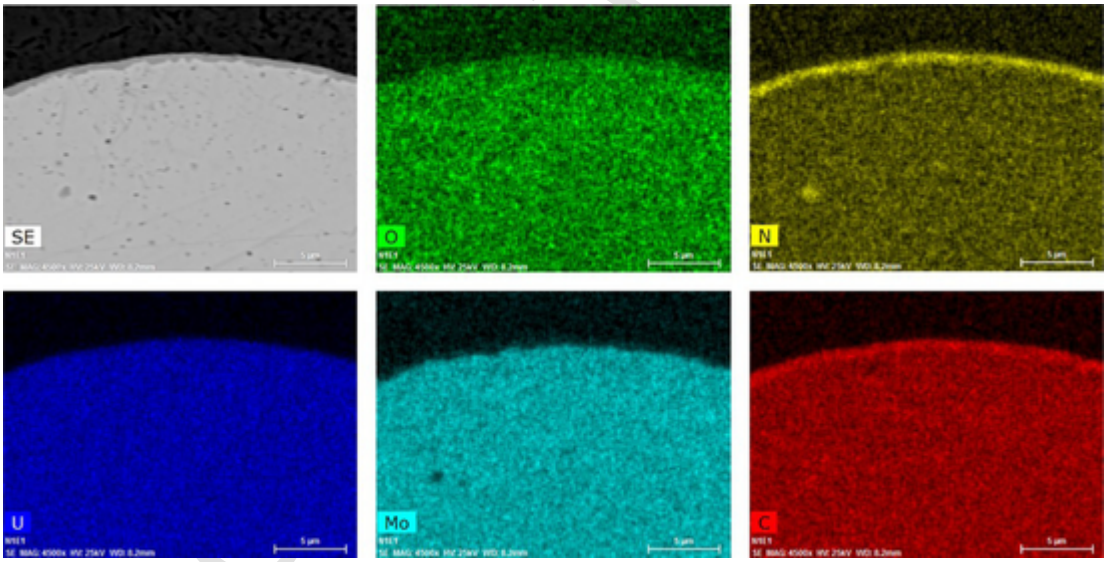

Fig. 3. Secondary electron image, O Kα, N Kα, U Mα, Mo Lα and C Kα x-ray distribution mappings of the outer surface of an annealed U(Mo) fuel particle.

4.3. Fuel plates

All fuel plates were manufactured by FRAMATOME-CERCA using their classical picture frame technique and hot rolling. The Zr Lα X-ray distribution map (Fig. 5a) obtained by electron probe microanalysis (EPMA) on the cross section of a fresh fuel plate, shows that for several particles the coating is damaged. As this was not observed in the examination of the as coated U(Mo), it is most probable that the damage results from the plate fabrication process. Fig. 5 shows that larger parts of the coating peeled off from the fuel particles surface. This type of damage is mostly observed at the interface between the meat and the cladding; and at those locations where fuel particles are in close contact with each other.

It should be noted that most of the ZrN flakes observed in the matrix and aligned parallel to the rolling direction, are the result of over-spraying in the coating process. During deposition ZrN will also be sputtered on the rotating drum. At a certain thickness, fragments will peel off the drum and will be pulverized by the tumbling U(Mo) powder. The resulting flakes are too small to be removed from the batch by sieving.

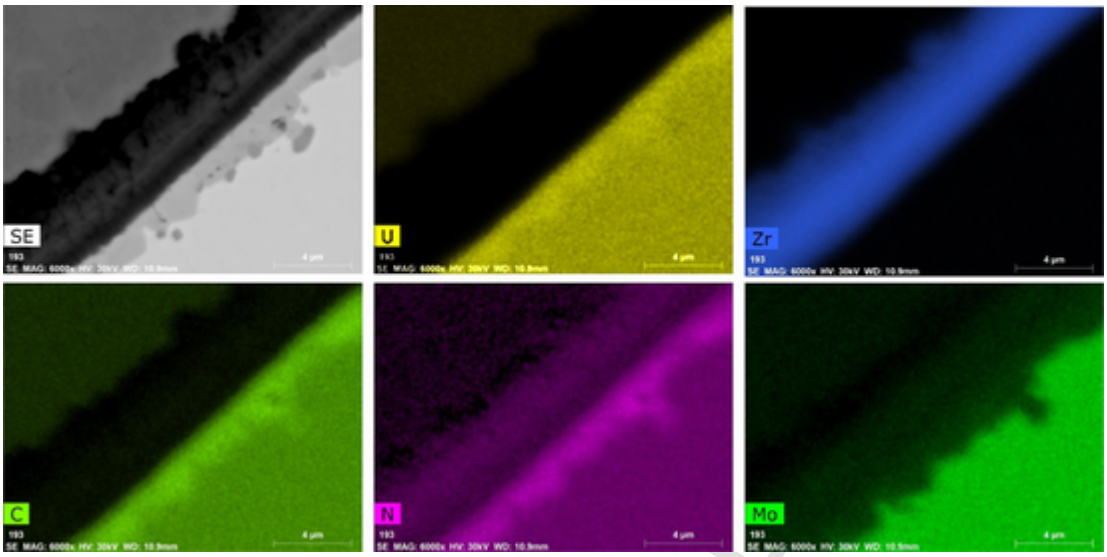

Fig. 4. Secondary electron image, U Mα, Zr Lα, C Kα, N Kα, and Mo Lα X-ray distribution mappings of the outer surface of a ZrN coated annealed U(Mo) fuel particle.

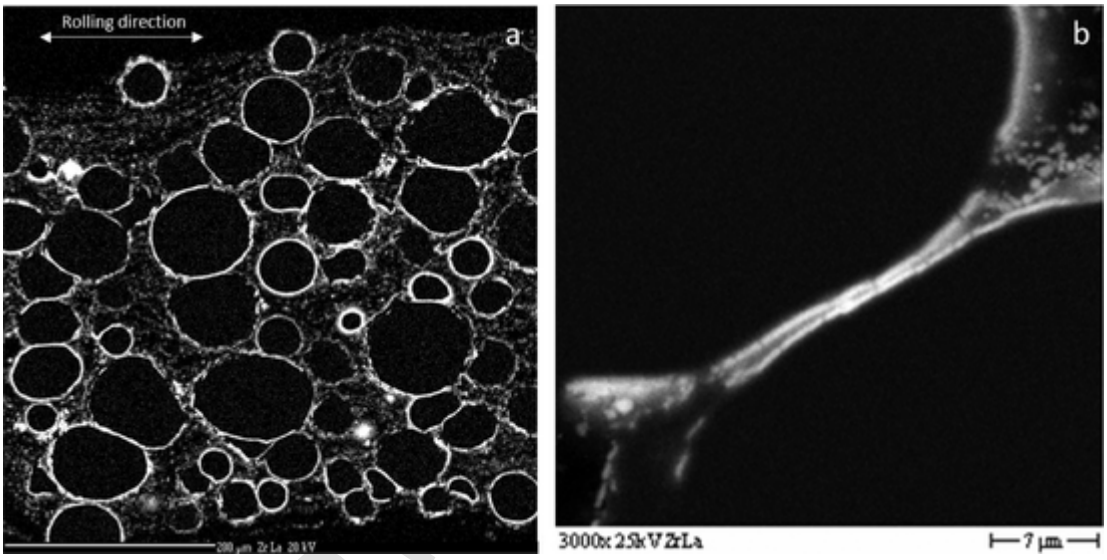

Fig. 5. Zr Lα X-ray distribution map : a) cross section of the plate showing the Zr flakes in the matrix and damage to the coatings b) detailed image of the coating on two adjacent U(Mo) particles, showing through thickness cracking.

The more detailed Zr Lα X-ray distribution map in Fig. 5b, reveals cracks in the coating, perpendicular to the U(Mo) surface. A thermal expansion mismatch between the fuel and the coating (thermal expansion coefficient for U10Mo (similar to the U7Mo used) is 11.5×10^{-6} m/m•K [27] and for ZrN is 7.24×10^{-6} m/m•K [28]) is, at least partly, the most probable reason. It causes the fuel to shrink more than the coating when cooling down after the heat treatment during plate production (hot rolling - blister test). The thermal expansion mismatch between coating and substrate results in tensile stress on the coatings in the radial direction and compressive strain in the tangential direction. It is the tensile stresses in the films that can cause through thickness microcracking [29]. However, the cracks may also result from the impact of mechanical forces (rolling) on the brittle, ceramic ZrN.

A third type of damage is the delamination of the ZrN coating (Fig. 6). Iltis et al. [30] showed that that this type of damage also has a preferential direction which is parallel to the rolling path. However, it was reported that this type of damage was mainly observed in the EMPIrE miniplates containing PVD ZrN coated particles, suggesting that the rolling conditions for miniplates are more severe compared to those applied on full sized plates.

5. The behavior of ZrN coating under irradiation

5.1. Microstructure

The evolution of the coating microstructure as a function of the fission density is illustrated in this paper through SEM analysis of polished and fractured surface samples.

Comparing the microstructure of the coating after irradiation to high burnup to the as fabricated coating (Fig. 1), the columnar, cauliflower structure can no longer be discerned (Fig. 7). Still some pores can be seen but it should be noted that their shape (rounded) differs from the pores seen at the column boundaries in the as fabricated layer (Fig. 1a). The contamination layer that has formed during the heat treatment (Fig. 4) on some of the U(Mo) kernel surfaces, seems to be

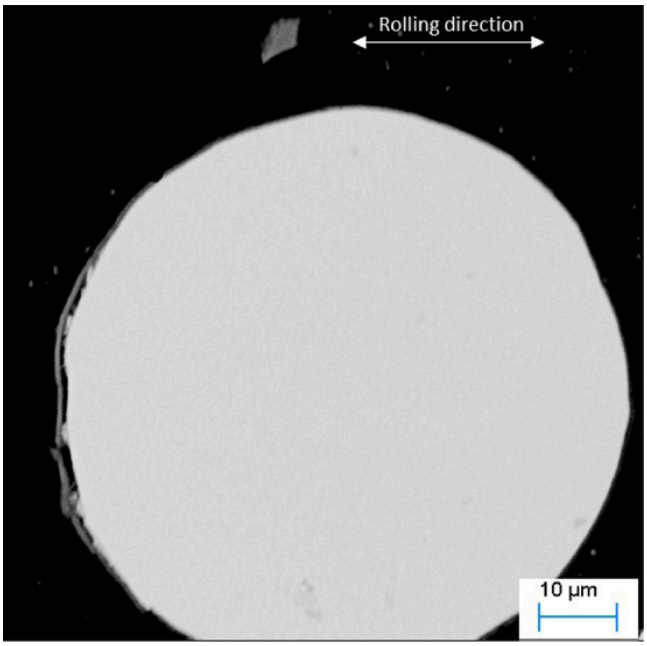

Fig. 6. Secondary electron image showing delamination of the ZrN coating.

unaffected and no interaction with the coating layer is observed (Fig. 7b)

The images in Fig. 7a,b also show that a layer in-between the coating and the Al matrix has formed. The formation of this layer is, similar to the formation of an interaction layer between the fuel and matrix, an ion driven diffusion process (ballistic effect) [18]. The images of the coating layer submitted to different burnups (Fig. 8), reveals that this interaction layer already forms at low burnup. Furthermore, it is noticed that with increased fission density the thickness of the coating layer is reduced while the coating-matrix interaction layer thickness increases.

Based on these SEM images, quantitative measurements were made of the thickness of the coating and interaction layers submitted to different fission density (Fig. 9).

In Fig. 9 an accelerated increase in the Al-Zr-N and related decrease of the ZrN layer thickness above ~4.5×10^{21}fissions/cc, is observed. A similar observation was also made for the growth of the interaction layer between U(Mo) and the Al matrix [31]. This transition behavior of the Al-U(Mo) IL growth around a threshold was related to the strong temperature dependence of the mixing rate between two materials under ion bombardment above a critical temperature [32,33]. It is apparent that a similar temperature dependence exists for neutron irradiated materials. By plotting the interdiffusion quantity as a function of irradiation temperature (based on calculations), the so called Q curve (Fig. 10) illustrates that the interdiffusion process is composed of an athermal regime and a temperature dependent regime. The transition temperature for a neutron irradiated Al-ZrN system between the two regimes is ~115 °C. Ion irradiation experiments on the Al-ZrN system are planned and the results will confirm or correct this threshold temperature.

By intentionally scratching the surface of the samples, the fractured surface of the grains becomes visible (Fig. 11). It shows a dense coating layer consisting of very small grains, with some in-between small (rounded) pores. The porous columnar structure as observed in the as fabricated coating, is no longer present which could indicate a restructuring (induced by fission fragments bombardment) of the ZrN layer.

The formed ZrN-Al intermixing layer (Fig. 11 pointed out by arrows) has a smooth appearance and a distinct and smooth boundary is observed between the remainder of the coating and the ZrN-Al interaction layer.

An extensive transmission electron microscopy (TEM) investigation by Van Renterghem et al. [34] reports that the irradiated ZrN coating has a polycrystalline structure with a grain size of the order of 100 nm. The observed ring diffraction pattern confirms that the coating crystal structure has an fcc symmetry in agreement with the ZrN structure reported in the ICSD database . The lattice parameter of the coating measured by electron diffraction is 4.64 ± 0.02 Å, which is in agreement with but above the 4.5773 Å reported in the reference database.

The structure of the ZrN-Al interaction layer was found to be polycrystalline and consisting of small grains of the order of 50 nm. The grains have an fcc crystal structure with a lattice parameter of 4.20 ± 0.02 Å. No specific phase could be attributed but it was suggested that a structure in-between pure Al (fcc with a = 4.056 Å) and $AlZr_3$ (cubic lattice with a ¼ 4.3917 Å and Al on the corner positions and Zr on the face centers) is most likely [34].

The study also showed that apart from the respectively de- and increase in layer thickness, the structure of the coating and interaction layer does not significantly change with burnup. More importantly, no interaction between the U(Mo) fuel and ZrN coating could be witnessed.

5.2. Elemental composition

The X-ray distribution maps of the main components of the coating, fuel and some of the fission products generated, were obtained by scanning transmission electron microscopy (STEM) and energy dispersive X-ray spectroscopy (EDS) [9]. From Fig. 12, a sharp interface between the U(Mo) and ZrN coating is seen as well as in-between the ZrN layer and the coating/matrix interaction layer. The fission products ejected out of the fuel kernel can be found incorporated in the ZrN coating, as

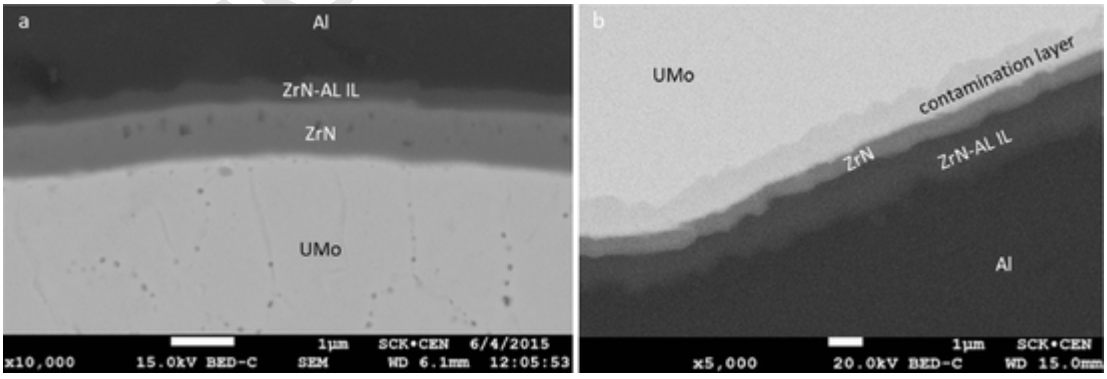

Fig. 7. Detailed back scattered electron images of an irradiated ZrN coated fuel particle at high burnup, in as polished condition. Both non-heat treated fuel particles (a) and heat treated particles (b) show the formation of a layer resulting from the interaction between the coating and matrix. Note the difference in magnification between the two images.

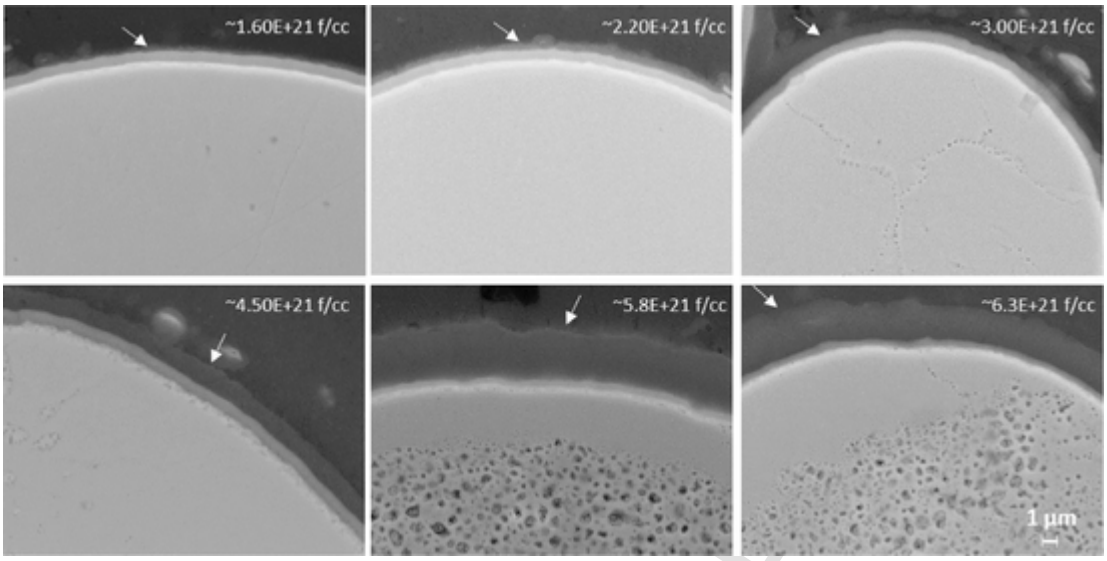

Fig. 8. Detailed secondary electron images of the intact ZrN coating submitted to different burnups. The formation of a layer in-between the coating an Al matrix is observed (pointed out by white arrow). The images are at the same magnification.

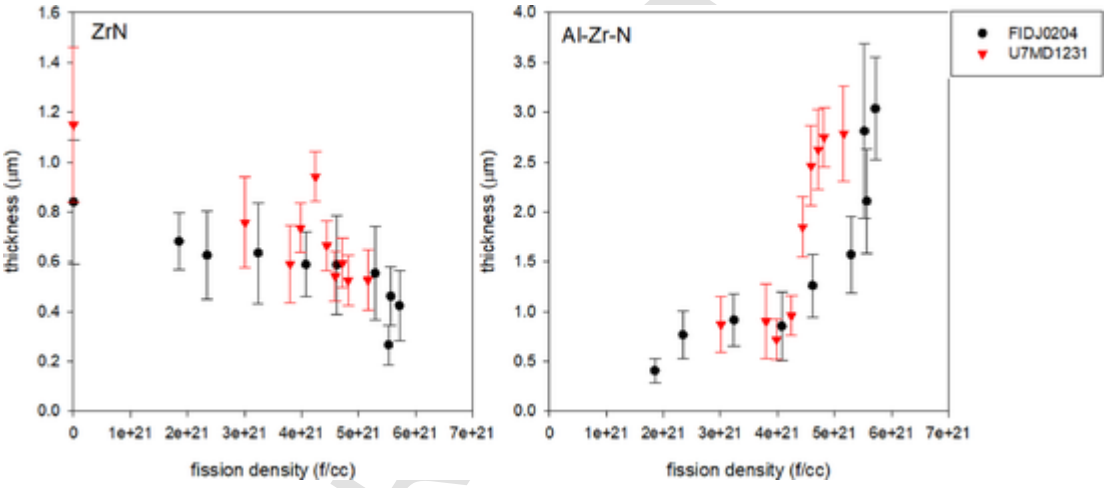

Fig. 9. Thickness of the ZrN coating layer (left) and the formed ZrN-Al interaction layer (right).

precipitates or in case of Xe as bubbles. This latter observation is consistent with the recording of rounded porosities in Fig. 7. Almost no fission products are found in the Zr-N-Al interaction layer but an accumulation of them, in particular Xe bubbles, at the interface of the coating/matrix interaction layer and the matrix is witnessed.

To obtain information on the composition of the interaction layer and coating, EPMA has been performed. When interpreting the data, one should keep in mind that the size of the measurement volume of the probe (electron beam) is comparable to the size of the coating. This means that in many cases no absolute values can be extracted for the composition and thickness of the interaction layer or coating. On samples that have received different burnups, several linescans covering the coating were defined, but also some manual measurements in point mode were obtained as reference. For all samples only Al, Zr, Mo and U were measured since it is very difficult to measure light elements such as nitrogen with EPMA. Nitrogen was introduced in the ZAF correction based on an assumption of stoichiometric ZrN, rather than on a measured result. The uncertainties associated to a measurement result of such a light element in these varying matrices (U(Mo), ZrN, Al) would be too large.

The results of the individual points and of the linescans are plotted in a pseudo ternary diagram (Fig. 13). If the coating would still be intact and had a width larger than the beam size, the points would form a perfect triangle. This is almost the case in the sample submitted to the lowest burnup (Fig. 13 black dots, 2.1 $\times$ 10^{21} f/cc). As the ZrN coating thickness decreases with increasing burnup, an apparent dilution of the coating with Al and U(Mo) could be related to the measurement conditions, i.e. a probe size larger than the coating thickness. The points encircled in red in Fig. 13, can be considered to reflect the composition of the layer resulting from the interaction between the ZrN coating and the Al matrix. The numerous compositions for the interaction layer found, confirms that the layer is induced by fission fragment induced intermixing and that no stable phase has formed.

A more accurate measurement of the coating and of the coating/matrix interaction layer was performed using atom probe tomography (APT) [9]. It was found that for a sample submitted to a burnup of 4.0 $\times$ 10^{21} f/cm^3, a nearly stoichiometric ZrN layer is measured (~56 at% Zr, ~44 at% N) indicating that the composition of the irradiated coating remains unchanged. A measurement at the interface between the ZrN coating and the Zr-N-Al interaction layer results in ~63 at% Al, ~36 at% Zr + N and ~1 at% U + Mo. At the interface between the Zr-N-Al and Al matrix a composition of ~85 at% Al, ~14 at% Zr + N and ~1 at% U + Mo was measured. The APT measurements are in line with the EPMA results (Fig. 13, pink stars).

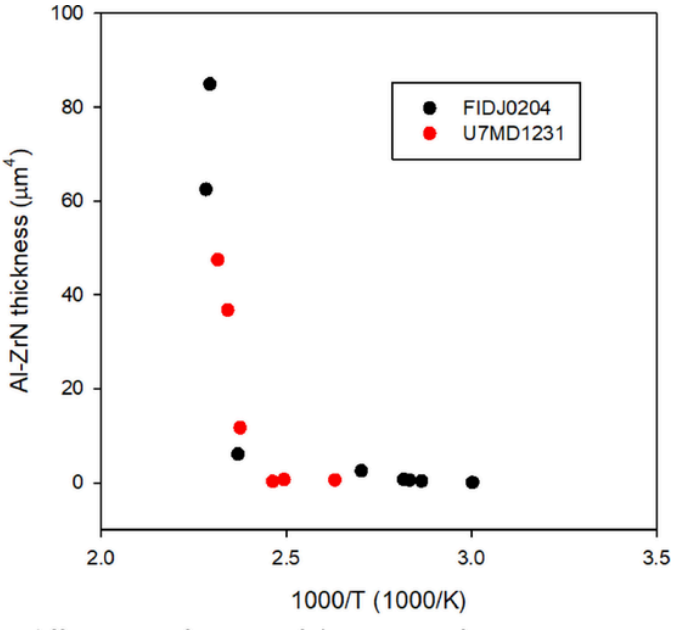

Fig. 10. Quantity of Al-ZrN interdiffusion as a function of the inverse of temperature.

5.3. Coating failure modes

The examination of the fresh fuel plates (4.3), shows three types of coating damage: large parts of the coating removed from kernel surface, through layer micro-cracks, and delamination of the coating.

As expected, at those locations where the U(Mo) fuel was in direct contact with the matrix, a U(Mo)-Al interaction layer has formed (indicated by a white arrow in Fig. 14a) [10]. Considering the low operating temperature of research reactors and similar to the ZrN-Al interaction layer, the formation of the U(Mo)-Al interaction layer is typically not thermally driven but is the result of a ballistic process [18] even if the transition to a much more thermal regime is reached at only slightly higher temperature [35].

The delamination of the coating from the fuel kernel surface does not seem to have an effect on the efficiency of the coating as a diffusion barrier. No formation of a U(Mo)-Al interaction layer can be observed (Fig. 14a, encircled in white).

For the through-layer micro-cracks, two evolutions are observed. It appears that if the crack was wide enough, the diffusion of Al through the crack has led to the formation of a U(Mo)-Al interaction layer (Fig. 14b). As irradiation, diffusion and intermixing progresses, the growing U(Mo)-Al interaction layer pushes the crack wider open as can be observed by the curled up coating at the edge of the interaction layer (Fig. 14b pointed out by a white arrow).

For the very small through-layer cracks, no diffusion of Al and subsequent formation of a U(Mo)-Al interaction layer can be observed (Fig. 14c). It appears that the small through-layer cracks get sealed off by the formed ZrN-Al interaction layer.

6. Improving behavior of the ZrN coating

From all neutron and ion irradiation experiments it has become clear that a ZrN coating on U(Mo) fuel kernels, acts as an efficient diffusion barrier up to very high burnup. Only at those locations where the coating is damaged and direct contact between the fuel and matrix occurs, a U(Mo)-Al interaction layer is formed. Even though this interaction layer only has limited effect on the observed fuel swelling, its amorphous character allows the diffusion of fission gas which collects at the interface of the interaction layer and the matrix. The subsequent large bubbles that form weaken the fuel plate integrity in such a way that breakaway swelling could occur.

As shown above, the damage of the coating is inherent to the fuel plate fabrication process (rolling, blister testing). As a remedy to restore the damaged coating, adding Si particles to the matrix was suggested.

The effect of silicon on the healing of the damaged ZrN coating, is based on the higher affinity of Si for U compared to the affinity of Al for U [36,37]. It is expected the Si in the matrix to interact, during plate production and subsequent irradiation, with the uncovered U(Mo) surfaces resulting in the formation of locally rich U-Si layers. However in previous irradiation experiments, based on U(Mo) dispersed in an Al-Si matrix [38–49] it was found that the use of Al–Si matrices could work if not for the inefficient diffusion of Si combined with the high U loadings. This results in an incomplete coverage of the kernels with a Si-rich preformed layer. Irradiation experiments with Si coated U(Mo) [4] confirmed the efficiency of U-Si rich layers as diffusion barrier and less interaction layer formation was seen, however at higher burnups crescent shaped porosities were observed at the interface of the coating and matrix.

In the SEMPER FIDELIS experiments, fuel plate FIDJ0301 consisting of ZrN coated U(Mo) dispersed in an Al-5%Si matrix (Table 3) was irradiated.

As both plates were fabricated in the same run and irradiated under the same conditions (Tables 2 and 4), direct comparison of the microstructure was possible.

As can be seen from the images in Fig. 15, at a burnup of approximately ~32% ^{235}U, the amount of interaction layer (colored green) is slightly higher for fuel plate FIDJ0203 compared to FIDJ0301. This difference becomes even more apparent at a higher burnup of ~42% ^{235}U.

From a more detailed X-ray distribution mapping (Fig. 16), the beneficial effect of adding silicon to the matrix and as such reducing the amount of interaction between the fuel and matrix, is clearly seen. Diffusion of silicon to uncoated U(Mo) particles (so called fines which are added to the meat to improve rolling) and the formation of a U-Si

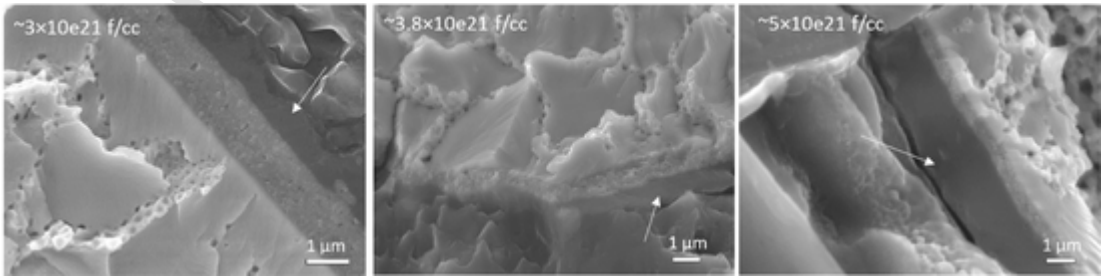

Fig. 11. Evolution of the ZrN coating observed in samples from fuel plate U7MD1231 (ZrN coated U(Mo)) on surfaces. The ZrN-Al interaction layer is pointed out by a white arrow. Please note the difference in magnification of the images obtained at the different burn-ups.

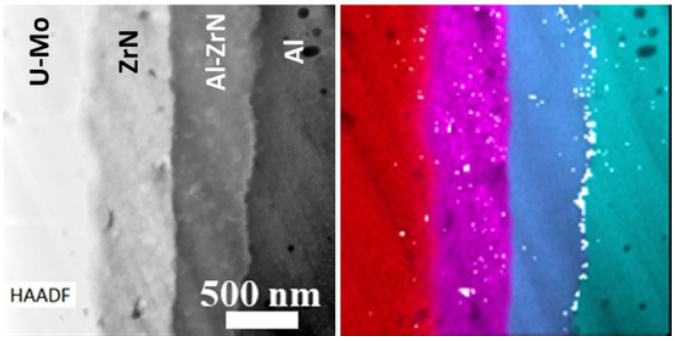

Fig. 12. STEM image and combined EDS maps showing element distribution of U (red), Zr (pink), Al (turquoise) and Xe (white). The individual and additional X-maps can be found in [9].

rich interaction layer is observed (indicated by encircled in 1Fig. 16). At the locations where a larger part of the ZrN coating is missing, a Si rich layer on the U(Mo) fuel surface has formed (indicated by encircled 2 in Fig. 16). Diffusion of silicon along the small through-layer cracks leads to the formation of a U-Si layer underneath the cracked ZrN layer (indicated by encircled 3 in Fig. 16)

7. Conclusions

The deposition of ZrN on U(Mo) particles using PVD results in the formation of a crystalline, stoichiometric ZrN coating that has a porous columnar, cauliflower microstructure consisting of small nano-sized grains. Analysis of the as fabricated coated fuel particles shows that the coating thickness is homogenous and fully covers the fuel particle surface. No interaction between the coating and the U(Mo) fuel or the contamination layer resulting from heat treating the fuel kernels, is witnessed. However, from the examination of the fresh fuel plates it is seen that damage to the coating during plate production is inevitable and could lead to unwanted interaction between the U(Mo) fuel and Al matrix.

Post irradiation examination shows changes to the structural integrity of the ZrN coating but confirms its efficiency as diffusion barrier up to very high burnup. Fission fragment induced intermixing creates an interaction layer between the ZrN coating and the Al matrix. The growth of this interaction layer is at the expense of the ZrN coating and the amount of interdiffusion shows a transition at 115 °C from temperature-independent to temperature-dependent behavior. The remaining ZrN coating and the formed ZrN-Al still exhibits a polycrystalline character and consist of smaller grains.

As expected, at those locations where the coating was damaged or missing, the formation of a U(Mo)-Al interaction layers was observed. As engineering solution for healing of the damaged coating adding Si to the matrix was proposed. An irradiation of a fuel plate consisting of ZrN coated fuel particles dispersed in a Al-Si matrix confirmed the beneficial effect as only a limited amount of U(Mo)-Al interaction layer has been observed.

At no point diffusion of Al through the ZrN coating was found, making this type of coating in combination with an Al-Si matrix, a less than the preferred solution for the successful irradiation of low enriched U(Mo) fuel plates.

CRediT authorship contribution statement

A. Leenaers: Conceptualization, Investigation, Writing – original draft. **B. Ye:** Formal analysis, Writing – review & editing. **J. Van Eyken:** Investigation, Formal analysis, Writing – review & editing. **S.**

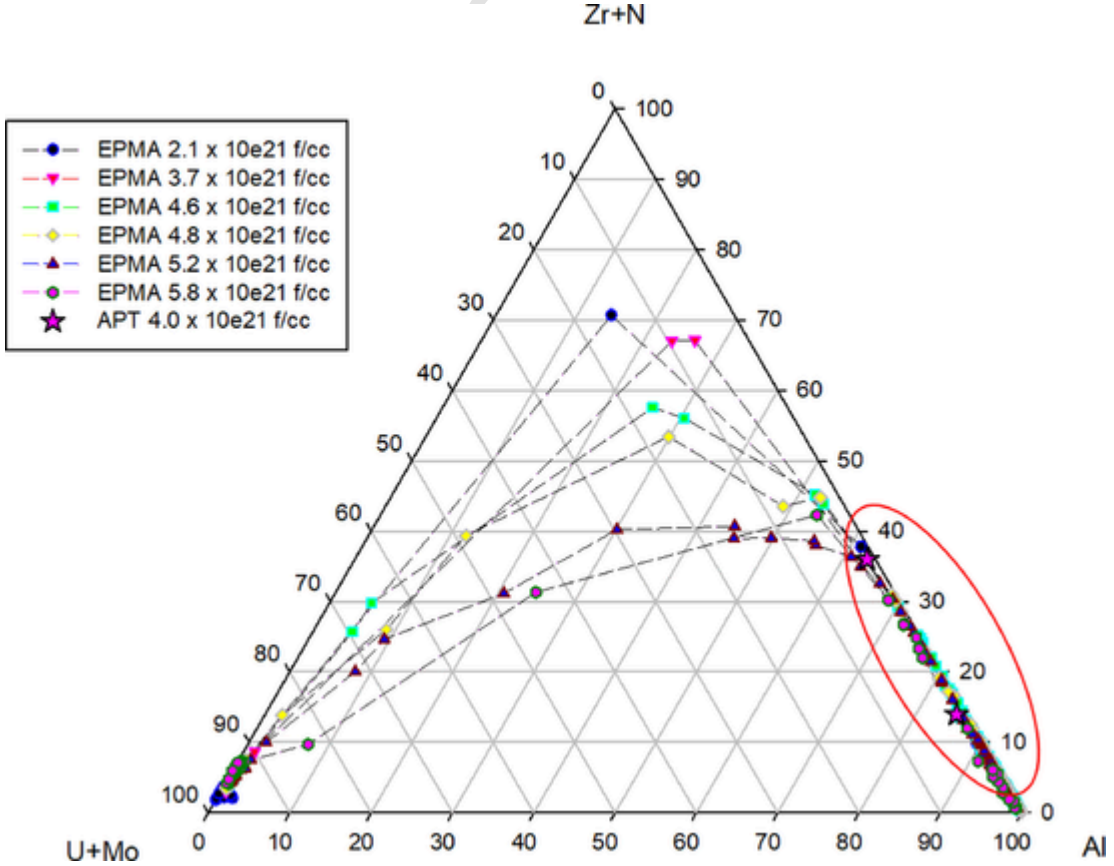

Fig. 13. Pseudo ternary diagram of Al, ZrN and U(Mo) (expressed in at%). The measurements of the interaction layer formed between the ZrN coating and the Al matrix, are encircled in red.

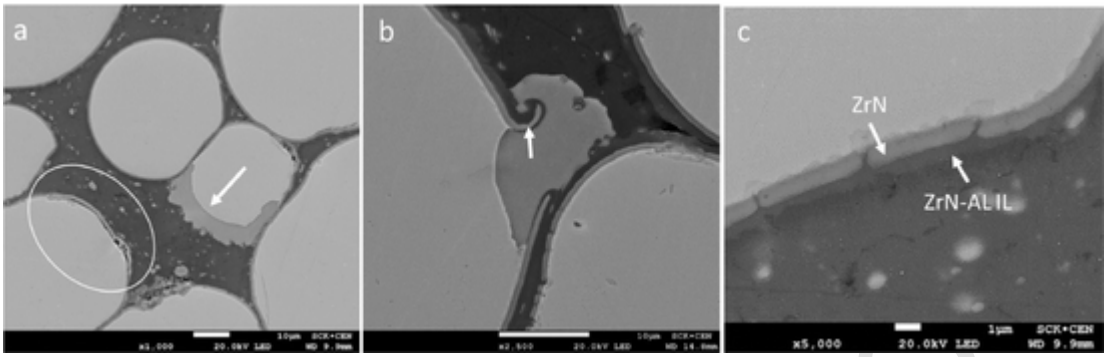

Fig. 14. Secondary electron images of irradiated ZrN coated U(Mo) fuel particles showing a) delamination of the coating b) volcano type of interaction layer c) through-layer cracks.

Table 3.
Fuel plate characteristics.

Experiment	Plate ID	Powder Type	Matrix Type	Coating thickness(μm)	Heat treatment of the U(Mo) particles
SEMPER FIDELIS	FIDJ0301	ZrN coated	Al + 5% Si	0.83 ± 0.23	HT

Van den Berghe: Conceptualization, Writing – review & editing, Funding acquisition.

Declaration of Competing Interest

The authors declare that they have no known competing financial interests or personal relationships that could have appeared to influence the work reported in this paper.

Acknowledgements

Argonne National Laboratory's work was supported by the U.S. Department of Energy, Office of Science, under contract DE-AC02-06CH11357.

Table 4.
Irradiation history of fuel plate FIDJ0301.

Experiment	Plate ID	Cycle	Max HF at BOCW/cm ^{2}	Max Burnup% ^{235}Uf/cc	Mean Burnup% ^{235}Uf/cc	EFPD
SEMPER FIDELIS	FIDJ0301	05/2017	526	35.8 2.6E + 21	22.9 1.6E + 21	28

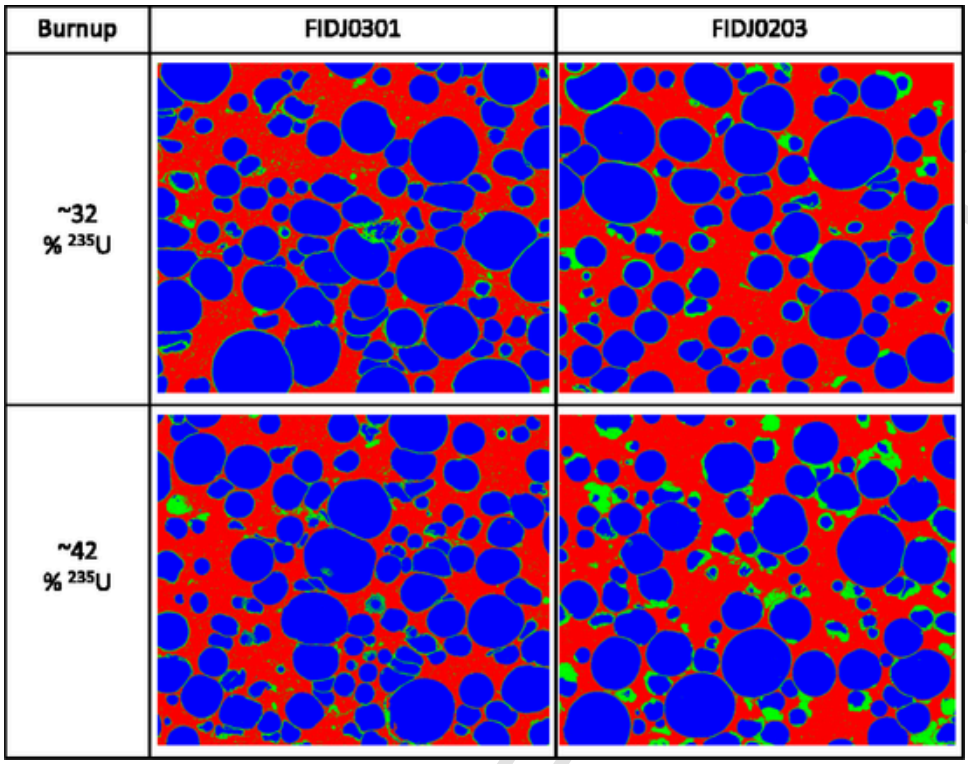

Fig. 15. Secondary electron images of the meat in fuel plates FIDJ0301 and FIDJ0203. To differentiate the separate phases present in the meat, coloring of the images is performed based on intensity thresholds (grey scale levels): fuel (blue), matrix (red), coating and interaction layer (green). (For interpretation of the references to color in this figure legend, the reader is referred to the web version of this article.)

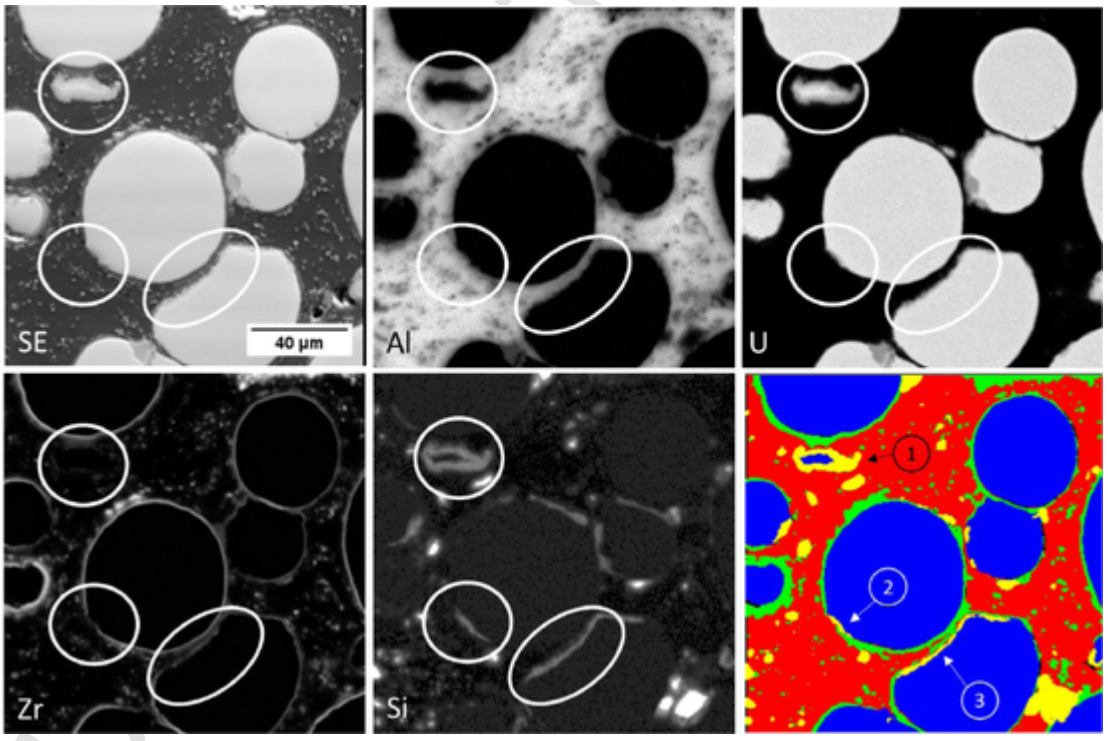

Fig. 16. Secondary electron image, Al Kα , U Mα , Zr Lα, and Si Kα blue x-ray distribution mappings of part of the meat: U Mα blue, Zr Lα green, Al Kα red and Si Kα yellow.

References

[1] A. Leenaers, S. Van den Berghe, C. Detavernier, J. Nucl. Mater. 440 (2013) 220–228.

[2] S. Van den Berghe, A. Leenaers, E. Koonen, L. Sannen, Adv. Sci. Techn. 73 (2010) 78–90.

[3] A.L. Izhutov, V.V. Alexandrov, N. A.E., V.A. Starkov, V.E. Fedoseev, V.V. Pimenov, A.V. Sheldyakov, V.Y. Shishin, V.V. Yakovlev, I.V. Dobrikova, A.V. Vatulin, V.B. Suprun, K. G.V., 32nd International Meeting on Reduced

Enrichment for Research and Test Reactors (RERTR), Lisbon, Portugal, Lisbon, Portugal, 2010.
[4] A. Leenaers, S. van den Berghe, E. Koonen, V. Kuzminov, C. detavernier, J. Nucl. Mater. 458 (2015) 380–393.
[5] T. Zweifel, H. Palancher, A. Bonnin, F. Charollais, A. Leenaers, S. Van den Berghe, R. Jungwirth, W. Petry, P. Lemoine, 16th International Meeting on Research Reactor Fuel Management (RRFM), Prague, Czech Republic, Prague, Czech Republic, 2012.
[6] T. Zweifel, H. Palancher, A. Leenaers, A. Bonnin, V. Honkimaki, R. Tucoulou, S. Van Den Berghe, R. Jungwirth, F. Charollais, W. Petry, J. Nucl. Mater. 442 (1–3) (2013) 124–132.
[7] D. Keiser Jr,, E. Perez, T. Wiencek, A. Leenaers, S. Van den Berghe, J. Nucl. Mater. 458 (2015) 406–418.
[8] Van Renterghem, W.; Leenaers, A.; Van den Berghe, S.; Miller, B. D.; Gan, J.; Madden, J. W.; Keiser, D. D., RERTR, Seoul,South Korea, Seoul, South Korea, 2015.
[9] L. He, M. Bachhav, D.D. Keiser, J.W. Madden, E. Perez, B.D. Miller, J. Gan, W. Van Renterghem, A. Leenaers, S. Van den Berghe, J. Nucl. Mater. 511 (2018) 174–182.
[10] B.D. Miller, D.D. Keiser, M. Abir, A. Aitkaliyeva, A. Leenaers, B.J. Hernandez, W. Van Renterghem, A. Winston, J. Nucl. Mater. 510 (2018) 431–436.
[11] S. Van den Berghe, Y. Parthoens, G. Cornelis, A. Leenaers, E. Koonen, V. Kuzminov, C. Detavernier, J. Nucl. Mater. 442 (2013) 60–68.
[12] R. Jungwirth, T. Zweifel, H.Y. Chiang, W. Petry, S. Van den Berghe, A. Leenaers, J. Nucl. Mater. 434 (2013) 296–302.
[13] S. Bhattacharya, X. Liu, Y. Miao, K. Mo, Z.-G. Mei, L. Jamison, W. Mohamed, A. Oaks, R. Xu, S. Zhu, J.F. Stubbins, A.M. Yacout, Acta Mater 164 (2019) 788–798.
[14] I. Glagolenko, N. Woolstenhulme, M. Lillo, J. Nielsen, D. Choe, J. Navarro, C. Jensen, D. Crawford, W. Jones, S. Snow, B. Hawkes, J. Wiest, D. Keiser Jr,, K. Holdaway, J.L. Schultness, B. Rabin, Proceedings of the European Research Reactor conference (RRFM), Berlin, ENS, Berlin, 2016.
[15] G. Hofman, L. Jamison, B. Ye, Z.-G. Mei, A. Yacout, A. Robinson, W. Hanson, J. Nielsen, D. Keiser Jr,, A. Leenaers, European Research Reactor Conference (RRFM), Online, ENS, 2020 Online.
[16] S. Bhattacharya, L. Jamison, D.N. Seidman, W. Mohamed, Y. Bei, M.J. Pellin, A.M. Yacout, J. Nucl. Mater. 526 (2019) 151770.
[17] C.K. Kim, J.M. Park, H.J. Ryu, Nucl. Eng. Technol. 39 (2007) 617–626.
[18] Leenaers, A.*Surface-Engineered Low-Enriched Uranium-Molybdenum Fuel for Research Reactors.* UGENT/SCK•CEN, Gent, 2014.ISBN-9789076971223
[19] G. Hofman, M.K. Meyer, A.E. Ray, 21st International Meeting on Reduced Enrichment for Research and Test Reactors (RERTR), São Paulo, Brazil, São Paulo, Brazil, 1998.
[20] R.J. Van Thyne, D.J. McPherson, Trans. Am. Soc. Met. 49 (1957) 598–619.
[21] D. Salvato, A. Leenaers, S. Van den Berghe, C. Detavernier, J. Nucl. Mater. 510 (2018) 472–483.
[22] A. Leenaers, W. Van Renterghem, S. Van den Berghe, J. Nucl. Mater. 476 (2016) 218–230.
[23] S.F. Meyer, J. Vac. Sci. Technol. 18 (1980).
[24] B.A. Movchan, A.V. Demchishin, Fiz. Metal. Metalloved 28 (1969).
[25] M. Ohring, Chapter 9 - Film Structure, in: M. Ohring (Ed.), Materials Science of Thin Films, Second Edition, Academic Press, San Diego, 2002, pp. 495–558.
[26] F. Housaer, F. Vanni, M. Touzin, F. Béclin, J. Allenou, A. Leenaers, A.M. Yacout, H. Palancher, B. Stepnik, O. Tougait, J. Nucl. Mater. 533 (2020) 152087.
[27] H.J. Ryu, J.M. Park, Materials Properties of U-Mo Fuel, 2012.
[28] J. Menghani, K.B. Pai, M.K. Totlani, Jalgoankar, World Congress on Engineering, London, UK, London, UK, 2010.
[29] V. Teixeira, Vacuum 64 (2002) 393–399.
[30] X. Iltis, H. Palancher, J. Allenou, F. Vanni, B. Stepnik, A. Leenaers, S. Van Den Berghe, D.D. Keiser, I. Glagolenko, EPJ Nuclear Sci. Technol. 4 (2018).
[31] B. Ye, Y. Miao, J. Shi, D. Salvato, K. Mo, L. Jamison, A. Bergeron, G.L. Hofman, A. Leenaers, A. Oaks, A.M. Yacout, S. Van den Berghe, W. Petry, Y.S. Kim, J. Nucl. Mater. 544 (2021) 152684.
[32] F. Rossi, M. Nastasi, M. Cohen, C. Olsen, J.R. Tesmer, C. Egert, J. Mater. Res. 6 (6) (1991) 1175–1187.
[33] R.S. Averback, Nucl. Instrum. Methods Phys. Res. Sec. B 15 (1) (1986) 675–687.
[34] W. Van Renterghem, B.D. Miller, A. Leenaers, S. Van den Berghe, J. Gan, J.W. Madden, D.D. Keiser, J. Nucl. Mater. 498 (2018) 60–70.
[35] B. Ye, G.L. Hofman, A. Leenaers, A. Bergeron, V. Kuzminov, S. Van den Berghe, Y.S. Kim, H. Wallin, J. Nucl. Mater. 499 (2018) 191–203.
[36] A. Leenaers, S. Van den Berghe, C. Detavernier, Solid State Sci. 14 (2012) 1133–1140.
[37] H.J. Ryu, Y.S. Kim, G.L. Hofman, J.M. Park, C.K. Kim, J. Nucl. Mater. 358 (2006) 52–56.
[38] S. Dubois, J. Noirot, J.M. Gatt, M. Ripert, P. Lemoine, P. Boulcourt, 11th International Meeting on Research Reactor Fuel Management (RRFM), Lyon, France, Lyon, France, 2007.
[39] G.L. Hofman, M.R. Finlay, Y.S. Kim, 26th International Meeting on Reduced Enrichment for Research and Test Reactors (RERTR), Vienna, Austria, Vienna, Austria, 2004.
[40] G.L. Hofman, Y.S. Kim, A.B. Robinson, 31st International Meeting On Reduced Enrichment For Research And Test Reactors, Beijing, China, Beijing, China, 2009.
[41] G.L. Hofman, Y.S. Kim, H.J. Ryu, J. Rest, D.M. Wachs, M.R. Finlay, 10th International Meeting on Research Reactor Fuel Management (RRFM), Sofia, Bulgaria, Sofia, Bulgaria, 2006.
[42] D.D. Keiser, J.F. Jue, A.B. Robinson, P. Medvedev, J. Gan, B.D. Miller, D.M. Wachs, G.A. Moore, C.R. Clark, M.K. Meyer, M.R. Finlay, J. Nucl. Mater. 425 (1–3) (2012) 156–172.
[43] Y.S. Kim, G. Hofman, A.B. Robinson, 13th International Meeting of Research Reactor Fuel Management (RRFM), Vienna, Austria, Vienna, Austria, 2009.
[44] Y.S. Kim, G. Hofman, H.J. Ryu, J. Rest, 27th International Meeting on Reduced Enrichment for Research and Test Reactors (RERTR), Boston, USA, November 6–10, Boston, USA, 2005.
[45] A. Leenaers, S. Van den Berghe, W. Van Renterghem, F. Charollais, P. Lemoine, C. Jarousse, A. Röhrmoser, W. Petry, J. Nucl. Mater. 412 (2011) 41–52.
[46] J.M. Park, H.J. Ryu, S.J. Oh, D.B. Lee, C.K. Kim, Y.S. Kim, G.L. Hofman, J. Nucl. Mater. 374 (3) (2008) 422–430.
[47] J.M. Park, H.J. Ryu, J.H. Yang, Y.S. Lee, B.O. Yoo, Y.H. Jung, H.M. Kim, C.K. Kim, Y.S. Kim, G. Hofman, 32nd International Meeting on Reduced Enrichment for Research and Test Reactors (RERTR), Lisbon, Portugal, Lisbon, Portugal, 2010.
[48] W. Petry, A. Röhrmoser, P. Boulcourt, A. Chabre, S. Dubois, P. Lemoine, C. Jarousse, J. Falgoux, S. Van den Berghe, A. Leenaers, 12th International Meeting on Research Reactor Fuel Management (RRFM), Hamburg (Germany), Hamburg (Germany), 2008.
[49] Ripert, M.; Dubois, S.; Boulcourt, P.; Naury, S.; Lemoine, P., 10th International Meeting on Research Reactor Fuel Management (RRFM), Sofia, Bulgaria, Sofia, Bulgaria, 2006.